Preparation and characterization of ceria magnesium aluminate nano powder for thermal barrier application

N Sankara Subaramainian[1], R Ramalingam[2,3] and M Vijayaraghavan[2,4]

[1] Thin film Research Laboratory, Department of physics, Thiagarajar College of Engineering, Madurai - 625 015, Tamilnadu State, India.
[2] Department of Mechanical Engineering, Thiagarajar College of Engineering, Madurai - 625 015, Tamilnadu State, India.

E-mail: [1] shankersathiya@yahoo.com , [3] ramalingamapk@gmail.com and [4] vijayaraghavantce@gmail.com

Abstract. The present work deals with the preparation of $CeMgAl_{11}O_{19}$ nano powder by sol gel citric acid route and to investigate its structural, surface and thermo-mechanical properties, to access its suitability for thermal barrier application. The XRD profile of the $CeMgAl_{11}O_{19}$ powder heat treated at different temperatures confirms polycrystalline structure. From the XRD data, mean grain size, lattice strain energy, dislocation density and other structural parameters have been investigated and reported. Thermal properties of the as synthesized $CeMgAl_{11}O_{19}$ powder have been studied from the TG-DTA and DSC measurement and the results are presented. Thermal conductivity of the $CeMgAl_{11}O_{19}$ specimen heat treated at different temperatures has been evaluated using the physical property measurement system and the results have been discussed. Hardness of the pelletized $CeMgAl_{11}O_{19}$ specimen heat treated at different temperatures has been measured in the Vickers scale and the results have been discussed. The influence of annealing temperature on the tensile strength and wear resistance of the $CeMgAl_{11}O_{19}$ specimen have been investigated and reported. The 2D and 3D AFM image of the $CeMgAl_{11}O_{19}$ specimen heat treated at 750^0 C shows the uniform surface pattern without any dark pits and pinholes. The surface roughness and grain size evaluated from the AFM data have been analyzed and presented.

1. Introduction

The concept of thermal barrier coatings (TBCs) is well-known among gas-turbine designers. The experimental results of thermal barrier coating indicate that the higher combustion temperature generated by adiabatic engine generally reduces the heat rejection rate [1]. The fundamental idea of a TBC is that an insulating ceramic top coat is used for thermal protection of components which are exposed to hot gas (*e.g.*, combustor linings, turbine guide vanes and turbine blades). Between the substrate and the top coat there is a bond coat, which is a metallic alloy [2]. In these days partially stabilized zirconia (PSZ), used as thermally insulating material on the piston crown face and reported a 19% reduction in heat loss through the piston [3]. Normally, the TBC system is required to have significantly increased phase stability, lower lattice and lower radiation thermal conductivity and improved sintering and thermal stress resistance under the engine high-heat flux and severe thermal cycling conditions. The development of low conductivity thermal barrier coatings requires test techniques that can accurately and effectively evaluate coating's thermal conductivity at high surface temperatures (typically at 1300 to 1400 °C). In particular hot section components of gas turbine

engines must function at peak efficiencies at 3000 ^{0} F to near stoichiometric temperature and at high pressure with minimal cooling and without degradation of component life [4]. Since this low thermal conductivity requires at high temperature environment, the evaluation of materials has to take initial and after certain thermal exposure. $CeMgAl_{11}O_{19}$ has been selected as TBCs material because of their ability to with stand at higher operating temperature, high temperature stability, high hardness, wear resistance and tensile strength at higher temperature, low cooling requirements and improved performance achievements.

2. Experimental procedure

The Sol-gel citric acid method was used for the powder synthesis of $CeMgAl_{11}O_{19}$. In Sol-gel citric acid method a stoichiometric amount of citric acid, about 1.2moles per mole of metals in the nitrate solution, was separately dissolved 500 ml of water. Appropriate amounts of cerium nitrate ($Ce(NO_3)_3.6H_2O$), Aluminum nitrate ($Al(NO_3)_3.9H_2O$) and magnesium nitrate ($Mg(NO_3)_3.6H_2O$) was dissolved in 1.2 molar aqueous citric acid solution. The entire mixture was well stirred in a magnetic stirrer at 90 °C. A viscous substance (sol) was formed in a short while from the start of the stirring action. Further stirring lead to the formation of a jelly layer and then a foam. This foam on further stirring resulted in the formation of an amorphous porous material, which on heating resulted in the formation of $CeMgAl_{l1}O_{19}$ crystallites, which was washed well and then ball milled for two hours, to get fine grained $CeMgAl_{l1}O_{19}$. The prepared $CeMgAl_{11}O_{19}$ powder material was annealed in the atmospheric condition between 400 °C and 900 °C for ten hours and then compacted into pellets of desired geometry. Thermal conductivity studies have been carried out using Techno four meter. The micro hardness testing of the specimen has been conducted in Vickers hardness scale, using Zwick micro-hardness tester.

3. Result and discussion

3.1. Structural analysis

The X- Ray Diffraction pattern of unannealed and annealed $CeMgAl_{11}O_{19}$ powder specimen at 300 °C and 750 °C is shown in the figure 1, The XRD profile of the entire $CeMgAl_{11}O_{19}$ powder specimen confirms the formation of the polycrystalline structure, constituted by nanocrystallites. The $CeMgAl_{11}O_{19}$ powder exhibits the amorphous state at the annealed temperature of 300 °C. The $CeMgAl_{11}O_{19}$ powder heat treated at 450 °C shows hexagonal structure with the preferred orientation along the (2 1 10) plane. The calculated lattice constants and all the orientations in the XRD profile are well in agreement with the standard JCPDS PDF data file number 04-010-0269 for $LaMgAl_{11}O_{19}$ Powder specimen. On the other hand the $CeMgAl_{11}O_{19}$ powder heat treated at 750 °C shows Cubic structure with the preferred orientation along the (1 1 1) plane. The other orientation observed corresponds to (220) and (311) plane.

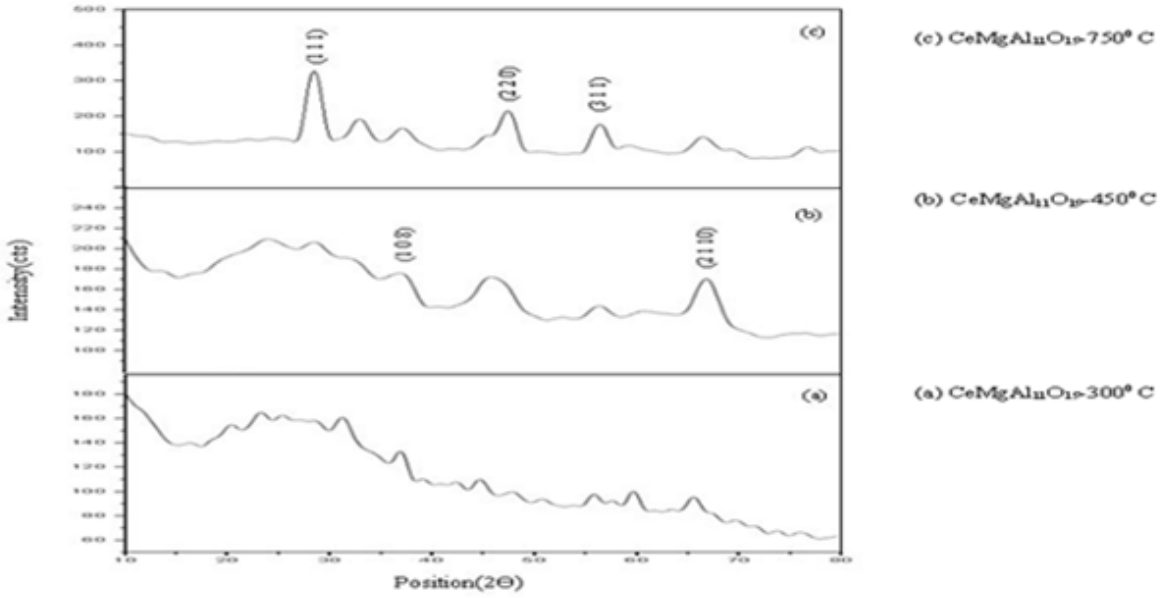

Figure 1. The XRD profile of $CeMgAl_{11}O_{19}$ powder

3.2. *Electrical Characterization*

Variation of resistance (R) and resistivity (ρ) of the pelletized $CeMgAl_{11}O_{19}$ specimen annealed at different temperatures is shown in the figure 2, The plot clearly illustrate that the R and ρ value increases, with the increase in annealing temperature and this may be attributed to the increased lattice scattering effect with the increase in the annealing temperature. The resistance and resistivity is found to be maximum with the value 6 MΩ and 9 x 10^{-6} Ω-cm respectively, for the $CeMgAl_{11}O_{19}$ specimen annealed at the temperature 750 °C.

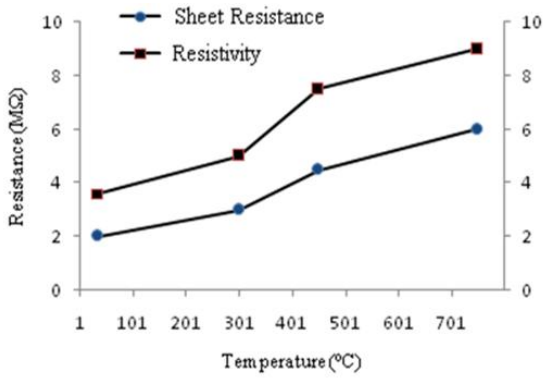

Figure 2. Variation of resistance and resistivity with annealing temperature

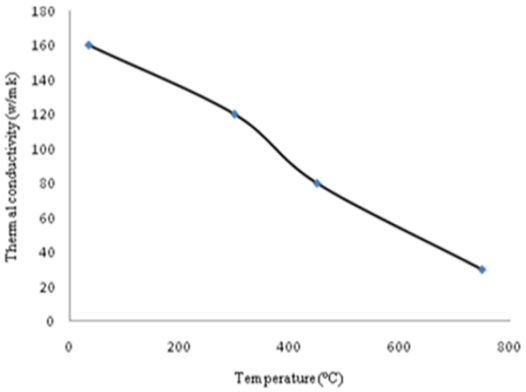

Figure 3. Variation of thermal conductivity with annealing temperature

3.3. Thermal conductivity studies

The thermal conductivity of pelletized $CeMgAl_{11}O_{19}$ specimen has been evaluated using the Wiedemann – Franz law stated below.

$$L = \frac{k}{\sigma t} \quad (1)$$

Where **L** is the Lorentz number (2.44 x 10^{-8} ΩW/K^2), **k** is the thermal conductivity in Watt /mK, **σ** is the electrical conductivity in mho / m and **T** is the absolute temperature in K. Using the above

relation, thermal conductivity of the unannealed sample have been estimated as 160 Watt / mK whereas for the pelletized $CeMgAl_{11}O_{19}$specimen annealed at different temperatures a steady fall in thermal conductivity have been observed. The variation of thermal conductivity as a function of annealing temperature is shown in figure 3, The plot shows a non – linear decrease in thermal conductivity with the increase in annealing temperature and this may be attributed to the micro structural variation and gradual raise in thermal diffusivity with the increase in annealing temperatures. The thermal conductivity is found to be maximum with the value 160 W/mK for the unannealed $CeMgAl_{11}O_{19}$ specimen and a minimum thermal conductivity of 18 W/mK is evaluated for the $CeMgAl_{11}O_{19}$ specimen annealed at 750 °C.

3.4. Micro hardness Studies

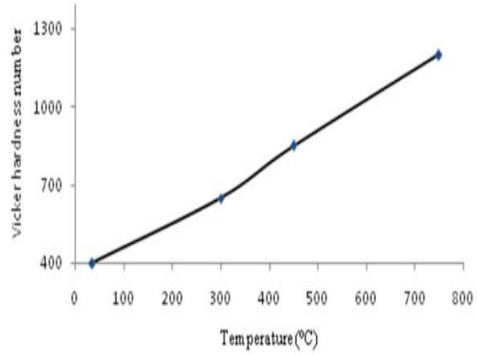

Figure 4. Variation of micro hardness with annealing temperature

The variation of VHN with annealing temperature of the $CeMgAl_{11}O_{19}$specimen is shown in the figure 4, The plot shows a non – linear increase in VHN with annealing temperature, indicating an improvement in the hardness of the films. This may be attributed to increase in the densification of compacted particulates at higher elevated temperatures, which ultimately increases the mechanical and thermal shock resistance of the $CeMgAl_{11}O_{19}$ specimen annealed at higher temperatures.. The hardness is found to be maximum with the value 1140 VHN and minimum with the value 400 VHN, for the $CeMgAl_{11}O_{19}$ specimen annealed at the temperatures 750 °C and unannealed specimen respectively.

3.5. Surface Characterization

The 2D and 3D AFM image of the pelletized $CeMgAl_{11}O_{19}$ specimen annealed at 450 °C and 750 °C are shown in the figure 5, and figure 6, respectively. The $CeMgAl_{11}O_{19}$ specimen annealed at 750 °C confirms the uniform distribution of fine grains throughout the surface without any dark pits and pin holes. The $CeMgAl_{11}O_{19}$ specimen annealed at 450 °C indicate more surface roughness and the presence of unevenly distributed coarse grains and small valley.

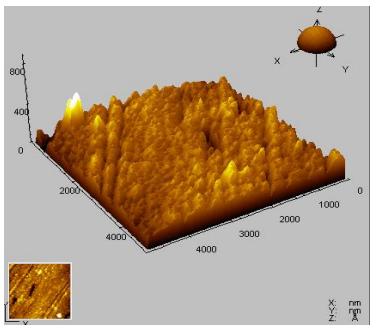

Figure 5(a). 3D AFM image of $CeMgAl_{11}O_{19}$ specimen annealed at 450 ºC

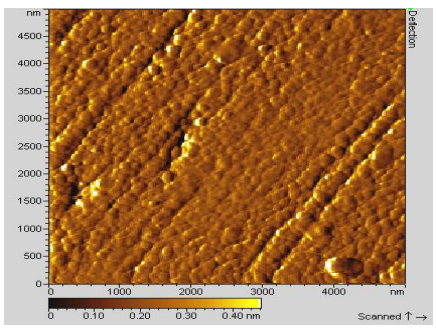

Figure 5(b). 2D AFM image of $CeMgAl_{11}O_{19}$ specimen annealed at 450 ºC

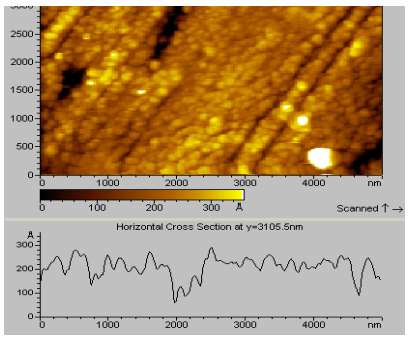

Figure 5(c). 2D AFM Roughness chart of $CeMgAl_{11}O_{19}$ specimen annealed at 450 ºC

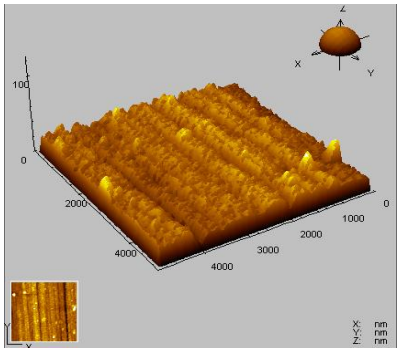

Figure 6(a). 3D AFM image of $CeMgAl_{11}O_{19}$ specimen annealed at 750 ºC

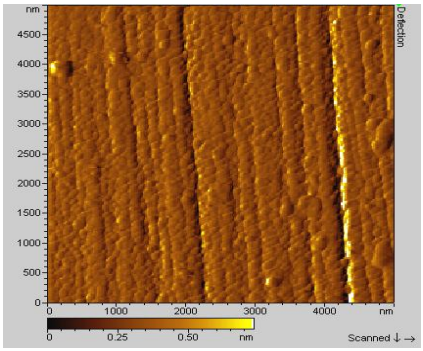

Figure 6(b). 2D AFM image of $CeMgAl_{11}O_{19}$specimen annealed at 750 ºC

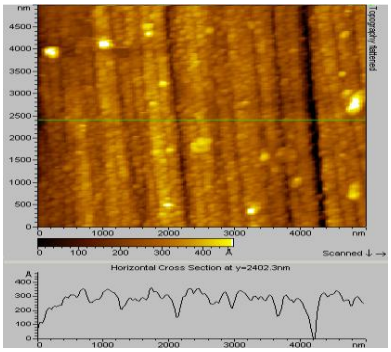

Figure 6(c). 2D AFM roughness chart of $CeMgAl_{11}O_{19}$ specimen annealed at 750 ºC

4. Conclusion

Ceria Magnesium aluminate ($CeMgAl_{11}O_{19}$) nano powder was prepared by sol-gel method. The $CeMgAl_{11}O_{19}$ powder heat treated at 450°C shows hexagonal structure with the preferred orientation along the (2 1 10) plane. On the other hand the $CeMgAl_{11}O_{19}$ powder heat treated at 750 °C shows cubic structure with the preferred orientation along the (1 1 1) plane. A sudden transition from the hexagonal to the cubic face is observed for the $CeMgAl_{11}O_{19}$ powder when annealed beyond the temperature 450 °C. The mean grain size evaluated from the XRD data lies between 16.5 nm and 44 nm. The resistance and resistivity is found to be maximum with the value 6 MΩ and 9 x 10^{-6} Ω-cm respectively, for the $CeMgAl_{11}O_{19}$ specimen annealed at the temperature 750 ^{o}C. Thermal conductivity of the $CeMgAl_{11}O_{19}$ specimen decreases non – linearly with the increase in annealing temperature and this may be attributed to the micro structural variation and gradual raise in thermal diffusivity with the increase in annealing temperatures. The thermal conductivity is found to be maximum with the value 160W/mK for the unannealed $CeMgAl_{11}O_{19}$specimen and a minimum thermal conductivity of 18W/mK is evaluated for the $CeMgAl_{11}O_{19}$ specimen annealed at 750 °C. The hardness is found to be maximum with the value 1140 VHN and minimum with the value 400 VHN, for the $CeMgAl_{11}O_{19}$ specimen annealed at the temperatures 750 °C and unannealed specimen respectively. The AFM micrographs of $CeMgAl_{11}O_{19}$ specimen clearly illustrate an increase in surface smoothness, grain boundaries, close packing of crystallites and grain size with the increase in the annealing temperature. The $CeMgAl_{11}O_{19}$ specimen annealed at 750 °C confirms the uniform distribution of fine grains without any dark pits and pin holes.

5. References

[1] Narottam P, Ohio D and Maryam E May 2007 Thermal properties of oxides with magnetoplumbite structure for advanced thermal barrier coatings. *NASA/TM* 214850.
[2] Gadow R and Lischka M 2002 Lanthanum hexaaluminate—novel tbc for gas turbine applications *Materials and Process Development. Surface Coatings Tech*. 151 to152. (2002) 392–399.
[3] Dongming Z and Miller A 2004 Development of advanced low conductivity thermal barrier coatings. *NASA/TM* (2004) 212961.
[4] Dongming Z and Miller A M 2002 Thermal conductivity and sintering behavior of advanced thermal barrier coatings. *NASA/TM* (2002)-211481.